Cement and Concrete Research 40 (2010) 752–762

Contents lists available at ScienceDirect

Cement and Concrete Research

journal homepage: http://ees.elsevier.com/CEMCON/default.asp

Linear and non-linear analysis of desorption processes in cement mortar

Halina Garbalińska [a], Stefan J. Kowalski [b,*], Maciej Staszak [b]

[a] West Pomeranian University of Technology, Faculty of Civil Engineering and Architecture, Aleja Piastów 50, 70-311 Szczecin, Poland
[b] Poznań University of Technology, Institute of Technology and Chemical Engineering, pl. Marii Skłodowskiej Curie 2, 60-965 Poznań, Poland

ARTICLE INFO

Article history:
Received 25 July 2008
Accepted 9 December 2009

Keywords:
Drying (A)
Humidity (A)
Diffusion (C)
Transport properties (C)
Mortar (E)

ABSTRACT

Based on the gathered experimental data concerning adsorption/desorption processes in cement mortar, it has been stated that the rate of these processes changes in time even if they proceed in stable conditions. In this paper an attempt is made to describe such processes by applying linear and non-linear diffusion theories for comparison. The main aim of these studies is to determine the diffusion coefficient by correlating the theoretically determined desorption isotherms with the experimental ones. The validation of the diffusion coefficient was accomplished through comparison of the theoretical desorption curves with the experimental data for narrow and broad ranges of the air humidity changes. The final conclusion is that the moisture transfer in hygroscopic porous materials for broad ranges of the air humidity changes should be modeled by the non-linear diffusion theory, in which the diffusion coefficient is a function of moisture content. The new material in this paper concerns very long time measurements in desiccators, and evaluation of the diffusion coefficient by an advanced optimization algorithm.

1. Introduction

Building materials like cement mortar are qualified as porous highly hygroscopic media, [1]. Being dry, they soak moisture from humid air, and conversely, being moist, they give the moisture back to dry air. The moisture transfer consists of three stages: the adsorption/desorption at the solid/gas interface, the moisture diffusion inside the pores, and the convective exchange of vapor between the porous material and the ambient air. The rate of this process varies in time, even if the external conditions provoking it are stable. This means that the diffusion rate changes accordingly to the moisture content in the material.

The objective of this paper is to provide a description of moisture transport inside the cement mortar by applying a linear diffusion model for narrow ranges of the air humidity changes and a non-linear diffusion model for both narrow and broad ranges of the air humidity changes for comparison. In particular, the paper presents a proposal for determination of the effective coefficient of diffusion D_{eff} on the basis of experimental adsorption–desorption measurements in cement mortar and application of an advanced optimization algorithm. The effective coefficient of diffusion expresses combined moisture transport, which occurs in both the adsorbed liquid and the gas phases present in the capillary-pore space.

In earlier works, a linear diffusion theory with constant diffusion coefficient D was applied for description of drying concrete elements, [2–5]. The values of determined coefficients D show a wide diversity ranging from $1.1\cdot10^{-12}$ to $1.6\cdot10^{-9}$ m^2/s [6].

Dependence of the diffusion coefficient on moisture content $D=D(C)$ was considered for first time by Pihlajavaara in [7]. He carried out a series of experiments concerning drying of concrete balls and cement mortar samples in the form of prisms, and attempted to describe these processes on the basis of diffusion theory. In the first approach he proposed a linear dependence of the diffusion coefficient on moisture content. However, his further studies did not confirm utility of such a linear function for greater values of moisture contents than $0.5\div0.6$. He proposed next in [8] a power function, which allowed to describe satisfactory the transport of moisture for moisture contents $C<0.9$. The values of the diffusion coefficient for the examined by Pihlajavaara samples ranged between $D=1.5\cdot10^{-11}$ and $D=20\cdot10^{-11}$ m^2/s.

The power function for the diffusion coefficient proposed by Pihlajavaara was critically reviewed by Bažant and Najjar [9,10], who did not confirm its usefulness in many cases. They undertook their own studies and interpolated this coefficient with air relative humidity and, additionally, with temperature and degree of hydration. They, as well as Hancox [4], utilized the new form of the diffusion coefficient and analyzed the drying processes of geometrically simple samples like spheres and plates made of concrete, mortar or gypsum. Their studies confirmed a good adherence of the theoretical and the experimental results.

Vos [11] constructed function $D(C)$ based on the measurements of the electric capacity of gas–concrete at various moisture contents. Van

* Corresponding author.
E-mail addresses: halina@zut.edu.pl (H. Garbalińska), stefan.j.kowalski@put.poznan.pl (S.J. Kowalski), maciej.staszak@put.poznan.pl (M. Staszak).

0008-8846/$ – see front matter © 2009 Elsevier Ltd. All rights reserved.
doi:10.1016/j.cemconres.2009.12.005

der Kooi [12] constructed function $D(C)$ based on measurements of electric resistance of gas concrete at various moisture contents. In each case, the magnitude of the diffusion coefficient changed by about several orders for a wide range of the moisture content variability.

Kiessl and Gertis [13] implemented function $D(C)$ proposed independently by Vos and Van der Kooi in the mathematical model of diffusion applied for analysis of drying of gas concrete plates. They determined charts of moisture distribution and showed clearly different mappings of the same processes as quantitatively as qualitatively, in spite of a similar range of variability moisture content in both cases.

The problem of liquid transport in building materials was examined in a broader context within the framework of the HAMSTAD project (Heat Air and Moisture Standards Development) [14]. The aim of the project was to propose an adequate modeling methodology for liquid water transfer in building materials. The results are published in four papers [15–18]. However, the theory presented by these researches has a number of limitations. The main one is its uncertainty in the low moisture content range, where combined liquid water and water vapor transport occur.

This paper concerns examination of moisture transfer in cement mortar just in the low moisture content range. A number of desorption isotherms at temperature $T=20$ °C were established for cement mortar samples with water/cement ratio $w/c=0.50$, for five narrow relative air humidity φ changes: 97%→85%, 85%→75%, 75%→50%, 50%→30%, 30%→12%, and for the broad relative air humidity φ change 97%→0%.

First, an attempt was made to adjust the theoretical desorption curves to the five narrow ranges of the air humidity change on the basis of a linear diffusion model. In the next step a non-linear model with the diffusion coefficient dependent on moisture content $D_{\text{eff}}(C)$ was adopted for analysis of both the narrow and the broad ranges of the air humidity change. The validity of this non-linear diffusion model was supported by a good conformity between the theoretical desorption isotherms and the experimental ones. The correlation of the theoretical predictions with the experimental data supported the hypothesis that the non-linear diffusive model reflected the moisture transport inside the hygroscopic porous material very well.

In this paper, the procedure for determining D_{eff} is significantly different from those described in references [1,15,19–25]. The solution of the linear diffusion equation is performed in the form of eigenfunctions series. The non-linear diffusion equation with a variable diffusion coefficient $D_{\text{eff}}(C)$ is solved, using the methods of lines. The linear and non-linear solutions are correlated with the experimental desorption isotherms by using a modified iterative algorithm of Levenberg–Marquardt [26]. The accuracy of the correlation is determined by applying the method of least squares and the stochastic polytope algorithm.

2. Description of the research part

2.1. Experimental background

The former researches conducted by Garbalińska within the framework of work [20] concerned determination of moisture diffusion coefficients through stationary measurements performed with the Cup Method (described in more detail in [27,28]) and through non-stationary adsorption and desorption measurements — using for calculations the logarithmic procedure and the √t-type procedure [19,29,30]. Moreover, a comparative analysis was conducted for the transport coefficients determined through the stationary processes with the Wet-Cup Method and the Inverse-Wet-Cup Method [31]. Subsequently, measurements of the capillary transport coefficients were taken, confronting in Ref. [32] the adapter method with the traditional capillary suction technique, which was described in more detail e.g. in Ref. [33]. Each of those tests was conducted in three temperatures: $T=20$ °C, 35 °C, 50 °C, and cement mortars with diversified water–cement ratios: $w/c=0.50$, 0.65, 0.80 were used as the object of the study.

For preparation of all the mixes, the same initial components were used: pure Portland cement and quartz sand ($0\div2$ mm) composed of individual fractions — in identical proportions. This approach ensured invariability of the contents and, as a result, guaranteed homogeneity of all individual mortars.

The cement–sand proportions were fixed in such a way that in each of the three mortars the ratio of the cement paste as a matrix to the aggregate as an inclusion was uniform: $(V_C+V_W)/V_A=\text{const}$. Meeting this condition guaranteed that each mortar could characterize with the same relation of volume of the matter, in which the moisture transport processes occur (cement paste), and volume of the matter, for which these processes can be recognized as meaningless (sand grains). If we consider the fact that moisture migration may also take place on the contact surface of the both element (cement paste-aggregate), maintenance of the above mentioned relationship ensures also identical contact surface in each of the mortars. One must note that the microstructure of hydrated cement paste, in a direct proximity of aggregate grains, features higher porosity, comparing to the microstructure of internal layers of grout. Although, according to Neville [34], in case of fine aggregate, extent of the contact layer is relatively small.

For all the three formulas, an identical component mixing technique was applied – the same as for production of the reference mortar [35]. Samples were made in cylindrical cast-iron forms with internal dimensions of $\varphi=8$ cm (diameter) and 16 cm (height). Compacting technique was adapted to the consistence. For the mix with $w/c=0.50$, mechanical compacting was used. For two other mortars, manual compacting was applied, by the means of a tool, built specially for that purpose, that guaranteed repeatability of the procedure for all samples of the given mortar.

Immediately after preparation, the samples were carried in their moulds to a chamber with temperature of about 20 °C and air relative humidity reaching 100%, where they remained for 24 h. Next, the samples were removed from the moulds and placed in water bath. Keeping them in water bath was recognized as necessary to be able to accept that in the samples concerned hydration processes ceased and that structural processes became stable.

Progress of the hydration process was ascertained by the means of derivatographic methods, described in more detail in Ref. [21]. Considering the fact that between the 12th and 24th month of curing growth of hydration degree achieved in the most unfavorable case (at $w/c=0.50$) only 3.3% — one-year-long water bath was accepted as sufficient for stabilizing the structures in the mortars used in this program.

It needs to be emphasized that the research program [20] was conducted for several years, therefore some of the samples were included in the testing procedure in the second year after their preparation, whereas other ones were included after 2, 3 or more years.

Within the framework of testing usability of non-stationary methods for determination of diffusion coefficients, first of all, an experiment consisting of two experimental blocks cycles was performed, where the first block included fifteen adsorption cycles and the second cycle included fifteen desorption cycles.

For studies on diffusion coefficient with non-stationary methods, disc-shaped samples of 80 mm diameter and 10 mm height were used. They were made from ϕ8/16 cm cylinders produced accordingly to the description provided above.

In the period preceding commencement of the studies on adsorption, the cylindrical samples were made subject to mechanical processing. With a diamond saw and a special template, the cylinders of all the individual mortars were cut to ≈10 mm discs. In order to avoid effects caused by structural changes due to carbonization in the

next-to-surface area, a several-millimeter-thick layer of the material was cut off and discarded on both the flat sides. As a result, all the discs originated from the central parts of the cylinders. Then, the discs were ground on both sides, so that their thicknesses were same − 10 mm. Type of the grinder used ensured that a specified thickness ±0.1 mm was achieved and it guaranteed that the opposite surfaces were parallel.

After taking a preliminary inventory of the samples, their side surfaces were insulated. Good consideration was given to the problem of selection of appropriate waterproof insulation. Its good quality was a necessary condition for obtaining a one-direction flow of moisture in the disc samples and prevented appearance of an uncontrolled stream of moisture migrating between the sample side surface and the insulation — in case there is no tightness in the contact area. Having tested various solutions, moisture-hardening silicone was recognized as the best for this purpose. It showed good adhesive tendency to the materials tested and proper resistance to high temperatures.

Each mortar yielded 45 disc samples of ϕ80/10 mm — to be used firstly for adsorption and then for desorption measurements. Fig. 1 shows a view of the samples.

Before starting the adsorption measurements, the samples were dried up to constant mass. Next, they were placed at one of the predetermined temperatures, grouping the samples by three of each mortar at five specified air relative humidity φ conditions.

In adsorption measurement block, relative humidity intervals were tested as per the scheme $0 \rightarrow \varphi_i$ — where for $T = 20$ °C: $\varphi_i = 30\%$, 50%, 75%, 85%, and 97%, for $T = 35$ °C: $\varphi_i = 32\%$, 51%, 75%, 82%, and 96% , whereas for $T = 50$ °C: $\varphi_i = 31\%$, 47%, 75%, 83%, and 96%. Realization of the extensive experimental block consisting of 15 measurement cycles required a continuous monitoring of changes in the sample mass during adsorption processes, which followed different courses under those conditions. Using an inverse task, from these courses a transport parameter was determined for each of the mortars, as belonging to individual section of $0 \rightarrow \varphi_i$. After the tested mortar samples achieved adsorption balance condition in each of the 15 climates, the desorption test block was started. This one consisted of 15 cycles, too (five for each of the abovementioned temperatures), performed according to the $\varphi_i \rightarrow 0$ scheme. Desorption processes were initiated due to transferring the samples with moisture φ_i, stabilized in the first experimental block, to moisture $\varphi \approx 0\%$. Changes of the sample masses had been recorded until the samples dried up. Application of the inverse task helped to determine, on the basis of mapped courses, values of diffusion coefficients for each mortar, in relation to each temperature and each section of the $\varphi_i \rightarrow 0$ humidity that were examined.

The extensive experimental material we had collected indicated strong variability in the diffusion coefficient, depending on temperature and humidity. However, the manner of conducting the studies, encompassing wider and wider ranges of humidity Δφ, made it impossible to provide detailed reconstruction of changes in the diffusion coefficient along with humidity.

This made us conduct differently arranged non-stationary desorption studies on the diffusion coefficient, as described in Section 2.2. They were supplemented by the tests presented in Section 2.3, which were aimed at determining a desorption isotherm. Measurements described in this paper make for continuation of studies discussed in Section 2.1, and consist in development of application of the non-stationary method for measuring the diffusion coefficient in a porous material. Testing of achievable precision of description of moisture transport processes was provided for in this paper based on desorption processes, related to a chosen mortar with ratio $w/c = 0.50$ at temperature $T = 20$ °C.

2.2. Non-stationary desorption measurements

Contrary to the desorption measurements of diffusion coefficients described in Section 2.1, respective to wider and wider ranges of humidity $\Delta\varphi = \varphi_i \rightarrow 0$, a concept of studies, which helps to describe the variable value of the diffusion coefficient we face at different levels of relative humidity φ and thus, at different levels of moisture in the material is provided below.

The described below desorption studies were arranged in such a way that they referred to narrow and adjacent ranges of $\Delta\varphi_i$, covering almost entire range of hygroscopic moisture. The desorption processes, which are presented here, were performed at $T = 20$ °C in five narrow sections of $\Delta\varphi_i$ for ϕ80/10 mm cement mortar samples with $w/c = 0.50$, prepared as described in 2.1.

The diffusion coefficients, which had been determined through the inverted method and assigned to individual sections of $\Delta\varphi_i$, were used to describe the drying process covering almost entire range of hygroscopic humidity $\Delta\varphi = 97\% \rightarrow 0\%$, results of which came from the formerly conducted desorption measurements, presented in Section 2.1. Tested in the almost full hygroscopic moisture humidity, the samples were going from the high humidity condition $\varphi = 97\%$ (stabilized above saturated water solution of K_2SO_4) to a condition typical for humidity $\varphi \approx 0\%$ (stabilized with silica gel). The drying process was studied for almost 4 months. At that time, a desiccator containing mortar samples was kept in a thermostatic chamber, ensuring maintenance of steady temperature of 20 °C throughout the testing period. The measurements came down to systematic recording of changes in masses of individual samples. Initially, the changes were quite rapid, but with time they slowed down significantly. Fig. 2 shows a resultant graph, illustrating in a schematic way the course of the drying process at $\Delta\varphi = 97\% \rightarrow 0\%$. It depicts the registered average changes in all the samples, referred to their volumes, thus providing changes in concentration C^*_s, which takes place during this process.

Fig. 1. Photo of the cement mortar samples used in the experiments.

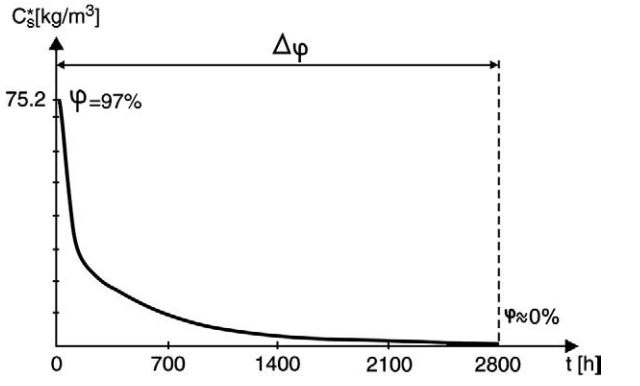

Fig. 2. Decrease of moisture content vs. time for the relative air humidity change $\Delta\varphi = 97\% \rightarrow 0\%$.

On the other hand, Fig. 3 provides changes in concentration C^*_s, recorded during the five desorption cycles in narrow-interval ranges of $\Delta\varphi_i$. The schematic courses juxtaposed on Fig. 3 make for products of studies conducted at $T=20$ °C on samples of the mortar with $w/c=0.50$.

On all levels, air relative humidity was stabilized with saturated water solutions of the salts: $\varphi=97\%-K_2SO_4$; $\varphi=85\%-KCl$; $\varphi=75\%-NaCl$; $\varphi=50\%-Ca(NO_3)_2$; $\varphi=30\%-CaCl_2$; and $\varphi=12\%-LiCl$. The basic experiments in five cycles of $\Delta\varphi_i$ followed an initial period when the ϕ80/10 mm mortar samples were reaching their moisture balance, appropriate for air relative humidity of $\varphi=97\%$. To this end they were kept long enough over solution of K_2SO_4. The main measurements in narrow-interval desorption cycles began on relocation of the samples from humidity of $\varphi=97\%$ to humidity of $\varphi=85\%$. In such humidity the samples remained until achieving a balance state. Next, they were put to the desiccator with solution of NaCl, i.e. to humidity of $\varphi=75\%$. Mass changes were recorded until their cessation. The stabilization of the mass was a signal to start another desorption cycle. The samples were transferred to a lower humidity of $\varphi=50\%$ and another cycle of drying and mass change recording began. After its completion, the samples were put into the desiccator with some $CaCl_2$ solution, and when the drying process in such conditions went down, the samples were placed above some solution of LiCl, where they remained until their moisture balance condition was achieved. So designed, the experiment consisted of five component cycles $\Delta\varphi_i$, carried out in the following order: $\Delta\varphi_1=97\%\rightarrow85\%$, $\Delta\varphi_2=85\%\rightarrow75\%$, $\Delta\varphi_3=75\%\rightarrow50\%$, $\Delta\varphi_4=50\%\rightarrow30\%$, $\Delta\varphi_5=30\%\rightarrow12\%$. Each time, in the thermostatic chamber (maintaining the temperature at 20 °C ± 1 °C), there was one desiccator with the volume of about 10 dm^3. On its bottom there was some hygrostatic solution, and inside of it, on special structures, 9 samples with total volume of about 450 cm^3 were placed. Realization of the 5-stage experiment lasted almost 1.5 year. During that period, beginning of each cycle required quite frequent measurements of the mass – within the first several dozen of hours, every 6 h, and later, every 12 h; then, after some time and when the recording process was not so intensive — once a day, to come ultimately down to once per several days. For each, cycle the measurements were finished when the mass changes (determined on the final stage in one-week intervals) achieved a level equivalent to the measuring scales precision.

It needs to be noted that the experiment of gradual going through all desorption cycles $\Delta\varphi_i$, taking several months, was burdened with uncontrolled effect of carbonization process. Unfortunately, it was not technically possible to remove CO_2 from the environment and exclude radically its participation in the recorded mass changes. However, considering results of tests performed by Kropp [36], it was understood that benefits from conducting the studies in each of the component cycles on the same samples prevail the minute inaccuracies resulting from the carbonization process.

The experimentally reproduced courses of mass changes during all the component cycles provided a base for determining through the invert task an effective diffusion coefficient for a given range of moisture in the material under study. Then, those diffusion coefficients, obtained from the individual ranges, were used to describe the general drying process within the range $\Delta\varphi=97\%\rightarrow0\%$, which played the role of a range testing usability and precision of the calculation procedures proposed in the paper. Their application required additionally a reconstruction of the desorption isotherm, which is described below.

2.3. Determination of the desorption isotherm

The results presented herein refer to the temperature $T=20$ °C and the cement mortar with ratio $w/c=0.50$. In order to determine the desorption isotherm presented on Fig. 4, samples obtained from cutting the ϕ80/10 mm discs to four equal pieces were used. All the sample surfaces participated in the moisture transport, and the main purpose was not to record the mass changes, but to determine the balance values. The samples were kept in seven air relative humidity conditions. Six identical humidity values and solutions as in Section 2.2. were adopted. Additionally, in order to increase density of the points on the desorption curve in the medium humidity area, a balance value for the air relative humidity of $\varphi=62\%$ was determined. For its stabilization, aquatic solution of saturated NH_4NO_3 was used.

Fig. 4 shows a desorption isotherm with indication of the spread of results obtained for value C_s.

3. Modeling approach

We assume that the process of moisture exchange between cement mortar and the surrounding atmosphere (air) is isothermal and diffusive in character. It can be divided into three stages: desorption of water particles adsorbed at the capillary wall, diffusion of vapor through the stagnant gas inside the mortar pores, and convective exchange of water vapor between the mortar and the ambient air.

Let us assume that a mortar samples (Fig. 1) consists of multiplicity of capillaries with radius R filled with moisture. Fig. 5a presents the geometry of the sample and Fig. 5b shows a single moisture-filled capillary, partly as vapor in air and partly adsorbed on the capillary surface.

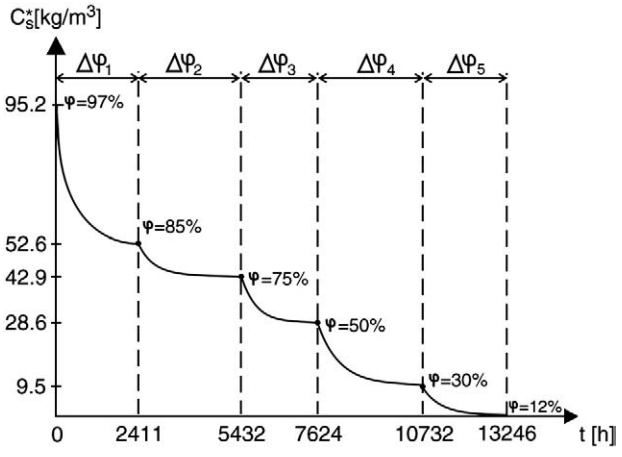

Fig. 3. Decrease of moisture content vs. time for the five short range processes of the relative air humidity change.

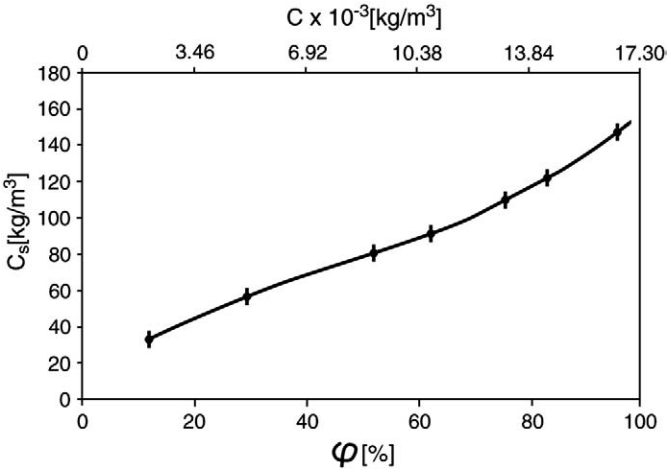

Fig. 4. Desorption isotherm for the cement mortar at $T=20$ °C.

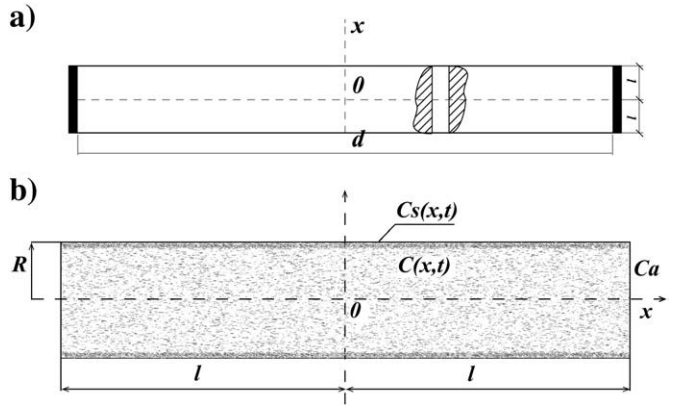

Fig. 5. Sample model: a) geometry of the sample, b) visualization of a capillary filled with moisture.

Let C_s [kg/m^3] be the adsorbed moisture content in the layer of thickness δ at the capillary wall and C [kg/m^3] the moisture content in air filled up the capillary space. We assume that the desorption rate is so high that the adsorbed moisture and the moisture in gas phases are in equilibrium in each cross-section of the capillary. According to this assumption, the rate of moisture removal from the capillary depends on the rate of mass transfer in both phases and between them. The starting point for constructing a differential equation describing this process is the balance of mass, in which the Fick's law is applied. For a single capillary, the balance of moisture mass reads [37]

$$\pi R^2 dx\frac{\partial C}{\partial t} + 2\pi R\delta dx\frac{\partial C_s}{\partial t} = \pi R^2 dx\frac{\partial}{\partial x}\left(D\frac{\partial C}{\partial x}\right) + 2\pi R\delta dx\frac{\partial}{\partial x}\left(D_s\frac{\partial C_s}{\partial x}\right) \tag{1}$$

where D [m/s^2] and D_s [m/s^2] denote the coefficients of diffusion in the gas and the adsorption phases respectively.

The boundary condition for the desorption process expresses the convective exchange of moisture between the mortar sample and the ambient air, namely

$$\pi R^2 D\frac{\partial C}{\partial x}|_{x=l} + 2\pi R\delta D_s\frac{\partial C_s}{\partial x}|_{x=l} = \pi R^2 k(C|_{x=l} - C_a) \tag{2}$$

where k denotes the coefficient of convective exchange of moisture (vapor), and C_a denotes the vapor content in the ambient air.

The symmetry conditions of moisture distribution in the capillary complete the set of boundary conditions

$$\frac{\partial C}{\partial x}|_{x=0} = 0 \quad \text{and} \quad \frac{\partial C_s}{\partial x}|_{x=0} = 0. \tag{3}$$

The initial conditions assume uniform distribution of moisture contents at the beginning of the desorption process

$$C(x,t)|_{t=0} = C_0 \quad \text{and} \quad C_s(x,t)|_{t=0} = C_{0s}. \tag{4}$$

Applying the desorption isotherm (Fig. 4)

$$C_s(x,t) = F[C(x,t)] \tag{5}$$

we can rewrite Eq. (1) and boundary condition (2) as follows

$$\left(1 + 2\frac{\delta}{R}\frac{\partial F}{\partial C}\right)\frac{\partial C}{\partial t} = \frac{\partial}{\partial x}\left(D_{\text{eff}}\frac{\partial C}{\partial x}\right) \tag{6}$$

$$D_{\text{eff}}\frac{\partial C}{\partial x}|_{x=l} = k(C|_{x=l} - C_a) \tag{7}$$

where D_{eff} is the effective coefficient of diffusion, being a combination the diffusion coefficients in gas and adsorption phases, that is

$$D_{\text{eff}} = D + 2\frac{\delta}{R}\frac{\partial F}{\partial C}D_s. \tag{8}$$

As the ratio of the adsorbed layer thickness to the capillary radius is very small, and the gradient of the desorption isotherm changeability with moisture content is a limited quantity, therefore, $1 \gg 2(\delta/R)(\partial F/\partial C)$ is assumed on the left side of Eq. (6) in further considerations. Thus, the final form of the diffusion equation reads

$$\frac{\partial C}{\partial t} = \frac{\partial}{\partial x}\left(D_{\text{eff}}\frac{\partial C}{\partial x}\right) = D_{\text{eff}}(C)\frac{\partial^2 C}{\partial x^2} + \frac{\partial D_{\text{eff}}}{\partial C}\left(\frac{\partial C}{\partial x}\right)^2. \tag{9}$$

Diffusion Eq. (9), boundary condition (7), symmetry condition $(3)_1$ and initial condition $(4)_1$ complete the system of equations for description of desorption processes between the mortar sample and the ambient air. As mentioned above, the experimental tests were carried out in such a way that the initial-boundary value problem can be considered for one-dimensional (Fig. 5a).

The cement mortar is assumed in this paper to be a rigid body. Therefore, the influence of the body deformation on the diffusion process is neglected. A more general theory of diffusion, including a material deformability, is presented, for example, in Refs. [38] or [39], and a more general discussion of moisture transport in deformable capillary-porous bodies during drying processes is presented in the monograph [40].

4. Linear diffusion

At first approach, we assumed that the amount of desorbed moisture and the non-uniformity in moisture distribution within the mortar sample at narrow ranges of the air relative humidity change were small. In such a case, the non-linear term in Eq. (9) can be neglected, and the diffusion coefficient should be considered as constant, but different in the individual intervals of the air relative humidity change. Thus, the diffusion of moisture for i-th interval (see Fig. 3) is described by the linear equation of the form

$$\frac{\partial C_i}{\partial t} = (D_{\text{eff}})_i\frac{\partial^2 C_i}{\partial x^2}. \tag{10}$$

Let us assume that the limit values of moisture content in the cement mortar are $(C_0)_i$ at the beginning and $(C_a)_i$ at the end of the i-th desorption process. During the process, the moisture content $C_i(x,t)$ is distributed along the sample height and changes in time from $(C_0)_i$ to $(C_a)_i$. In order to find the moisture distribution in the sample and its evolution in time, it is necessary to solve Eq. (10), applying the following boundary and initial conditions:

$$-(D_{\text{eff}})_i\frac{\partial C_i}{\partial x}|_{x=l} = k_i(C_i|_{x=l} - (C_a)_i), \quad \frac{\partial C_i}{\partial x}|_{x=0} = 0, \quad C_i|_{t=0} = (C_0)_i. \tag{11}$$

The boundary condition on the left determines the rate of desorption by the convective exchange of moisture between the sample and the ambient air. The second one expresses symmetry of moisture distribution within the sample with respect to the middle of the sample. The initial condition assumes a uniform distribution of moisture at the beginning of the i-th desorption process.

Using the method of variable separation for solution of the above initial-boundary value problem, one obtains the solution in the form of eigenfunctions series

$$C_i(x,t) = (C_a)_i + 4((C_0)_i - (C_a)_i)\sum_{n=0}^{\infty}\frac{\sin(\omega_n)_i}{2(\omega_n)_i + \sin 2(\omega_n)_i}\cos(\omega_n)_i\frac{x}{l} \times \exp\left(-(\omega_n)_i\frac{t}{(t_R)_i}\right) \quad (12)$$

where "$\cos(\omega_n)_i(x/l)$" are the eigenfunctions with the eigenvalues $(\omega_n)_i$ determined by the characteristic equation

$$\tan(\omega_n)_i = \frac{K_i}{(\omega_n)_i}. \quad (13)$$

The parameters $K_i = k_i l/(D_{\text{eff}})_i$ and $(t_R)_i = l^2/(D_{\text{eff}})_i$ appearing in Eqs. (12) and (13) are the two parameters of the theoretical solution, which are used for the correlation with experimental data.

The sample is a disc of diameter $d = 0.08$ m and height $2l = 0.01$ m. The mass of the desorbed moisture from the sample during i-th desorption process is described by the following integral

$$(m_m)_i(t) = 2A\int_0^l (C_s)_i(x,t)dx = (m_{am})_i + 4((m_{0m})_i - (m_{am})_i) \times \sum_{n=0}^{\infty}\frac{\sin^2(\omega_n)_i}{(\omega_n)_i(2(\omega_n)_i + \sin 2(\omega_n)_i)}\exp\left(-(\omega_n)_i\frac{t}{(t_R)_i}\right) \quad (14)$$

where $A = \pi d^2/4$ is the area of the disc face, $(C_s)_i = HC_i$ expresses a linear section of the desorption isotherm for the i-th narrow range of the air humidity change $\Delta\varphi_i$, $(m_{0m})_i = 2AlH(C_0)_i$ and $(m_{am})_i = 2AlH(C_a)_i$ denote the masses of moisture at the beginning and at the end of i-th desorption process, and H is the coefficient of proportionality between the adsorbed moisture content C_s and the moisture content in air C (Henry's constant).

In the experiments, the decrease of total sample mass $(\Delta m_t)_i = (m_0)_i - (m_t)_i(t)$ in time was measured, which is equal at the same time to the decrease of moisture mass $(\Delta m_m)_i = (m_{0m})_i - (m_m)_i(t)$. The experimental and theoretical results can be compared as follows

$$f_i(t) = 1 - \frac{(\Delta m_t)_i(t)}{(\Delta m_{\max})_i} = \frac{C_i(t) - (C_a)_i}{(C_0)_i - (C_a)_i} = 4\sum_{n=0}^{\infty}\frac{\sin^2(\omega_n)_i}{(\omega_n)_i(2(\omega_n)_i + \sin 2(\omega_n)_i)}\exp\left(-(\omega_n)_i\frac{t}{(t_R)_i}\right) \quad (15)$$

where $(\Delta m_{\max})_i = (m_0)_i - (m_a)_i$ denotes the maximum of sample mass decreased, equal to the maximum moisture mass removed from the mortar sample in i-th desorption process.

The correlation procedure requires a good choice of parameters K_i and (t_R), that is, parameters which give a "best" approximation to the function (15). Knowing these parameters, one can calculate the value of diffusion coefficient $(D_{\text{eff}})_i$ [m^2/s] and the coefficient k_i [m/s] influencing the diffusion rate.

5. Non-linear diffusion

The parameters of the experimental and theoretical curves for the non-linear diffusion model are again the coefficient of diffusion D_{eff} and the convective gas-side transfer k. The coefficient of diffusion D_{eff} is assumed to be a function of moisture content C, and takes the following form for both the narrow and the broad ranges of the air relative humidity change:

$$D_{\text{eff}}(C)_i = a_i\exp(b_i C) + c_i. \quad (16)$$

The coefficients correlated in this expression are given in Table 1.

The integration of the non-linear diffusion Eq. (9) was carried out by applying the method of lines (MOL) and using the MOLCH procedure from the IMSL package (see Ref. [41]). The basic idea of MOL is to replace the spatial derivatives in the differential equation with finite differences (FD), as for example

$$\frac{\partial C}{\partial x} \approx \frac{C_k - C_{k-1}}{\Delta x} \quad (17)$$

where k is the index designating a position along a grid in x, and Δx is the spacing in x along the grid. In the FD approximation of the spatial derivative (Eq. (17)) k involves C_k and C_{k-1}. In this system, C_{k-1} is to the left of C_k in x or is upstream or upwind of C_k. Thus, approximation presented by Eq. (17) is termed the first order upwind FD.

The complete MOL approximation of Eq. (9) is

$$\frac{dC_k}{dt} = D_{\text{eff}}(C)\frac{C_{k+1} - 2C_k + C_{k-1}}{\Delta x^2} + \frac{\partial D_{\text{eff}}}{\partial C}\left(\frac{C_k - C_{k-1}}{\Delta x}\right)^2 \quad \text{with } k = 1\ldots N. \quad (18)$$

The boundary and initial conditions expressed in FD take the form:

$$-D_{\text{eff}}\frac{C_k - C_{k-1}}{\Delta x}\Big|_{x=l} = k(C_k|_{x=l} - C_a), \quad \frac{C_k - C_{k-1}}{\Delta x}\Big|_{x=0} = 0, \quad C_k|_{t=0} = C_0. \quad (19)$$

The numerical solutions of the non-linear boundary value problem for all ranges of the relative air humidity change are derived, using the methods of lines. The numerical solution is correlated with corresponding experimental desorption isotherms, using the modified iterative algorithm of Levenberg–Marquardt [26]. Accuracy of the correlation is based on the least-squares method and on the stochastic polytope algorithm.

Table 1
Maximum and minimum values of the moisture content in several ranges of the air relative humidity change and the coefficients appearing in the analytical expression (16).

Cycle	max$C_i \cdot 10^{-3}$ [kg/m^3]	min$C_i \cdot 10^{-3}$ [kg/m^3]	a_i	b_i	c_i
97–85%	16.76	14.69	$1.879 \cdot 10^{-11}$	$3.9 \cdot 10^{-2}$	$-3.3 \cdot 10^{-9}$
85–75%	14.69	12.96	$6.986 \cdot 10^{-12}$	$5.3 \cdot 10^{-2}$	$-3.5 \cdot 10^{-9}$
75–50%	12.96	8.64	$5.915 \cdot 10^{-13}$	$8.9 \cdot 10^{-2}$	$-6.5 \cdot 10^{-10}$
50–30%	8.64	5.34	$1.08 \cdot 10^{-11}$	$8 \cdot 10^{-2}$	$-3.7 \cdot 10^{-10}$
30–12%	5.34	2.07	$1.174 \cdot 10^{-10}$	$1 \cdot 10^{-1}$	$-7.6 \cdot 10^{-10}$
97–0%	16.76	0.000	$4.923 \cdot 10^{-10}$	$2.7 \cdot 10^{-2}$	$-5 \cdot 10^{-10}$

6. Results and discussion

The experimental desorption tests carried out for the narrow intervals of the air relative humidity change constituted the basis for determination of the mean effective diffusion coefficient $(D_{\text{eff}})_i$. The modified iterative algorithm of Levenberg–Marquardt [26] and the polytope algorithm have been used to determine the two parameters K_i and $(t_R)_i$, which give the best approximation to the balance function (15). This way, mean coefficients $(D_{\text{eff}})_i$ for each of the five narrow intervals of the air humidity change were determined.

In the first approach, the Levenberg–Marquardt algorithm, applied by program UNLSF in the IMSL package, uses a least-squares procedure (see Ref. [42]):

$$\text{find:} \quad S = \min\sum_{k=0}^{\infty}[d_k(X_i)]^2 \quad \text{for} \quad d_k(X_i) = g_k - f_k(t, X_i) \quad (20)$$

where g_k are the experimental data and X_i denotes a two-dimensional vector consisting of components K_i and $(t_R)_i$. As the algorithm is iterative in character, it requires initial values for parameters K_i and $(t_R)_i$, then a loop procedure seems to be the best solution. The procedure is effective, provided that the successive approximations give a

sufficient decrease of residual values d_k of the functions f_k at successive iterations.

The stochastic polytope method of the second approach, applied by program UMPOL in the IMSL package, is based on the comparison of the function values (no function smoothness is necessary). This method is suitable for seeking minima of random functions or when the experimental data are dispersed. The computation of function minima is performed by using Nelder–Mead method, sometimes referred to as the simplex method. The algorithm applies this method for function minimization, and requires only function evaluations, not derivatives.

The simplex is a geometrical convex figure in n dimensions consisting of $n+1$ vertices X_i. In two-dimensional space X_i $[K_i, (t_R)_i]$, it is a triangle with 3 vertices. At each iteration, the values of the function at the vertices are compared, and a new point is generated to replace the point X_i, which has the highest function value. The new point is constructed by the following formula:

$$\overline{X}_i = A + \alpha(A - X_i) \quad \text{with} \quad A = \frac{1}{n}\sum_{j=1}^{n} X_j \tag{21}$$

where α ($\alpha > 0$) is the reflection coefficient. When the new point $\overline{X}_i$ is the best one, that is, when $d_k(\overline{X}_i) \le d_k(X_i)$ for $k = 1, \ldots, n+1$, an expansion point is computed $X_e = A + \beta(\overline{X}_i - A)$, where β ($\beta > 1$) is called the expansion coefficient. If the new point is worse than the former one, the polytope should be contracted to get a better new point. If the contraction step is unsuccessful, the polytope should be shrunk (narrowed) by moving the vertices halfway towards a current best point. This procedure is repeated until one of the following stopping criteria is satisfied, (see Refs. [43,44]).:

1. $f_k(t, X_{\text{best}}) - f_k(t, X_{\text{worst}}) \le \varepsilon(1 + |f_k(t, X_{\text{best}})|)$

2. $$\sum_{i=1}^{N+1}\left(f_k(t, X_i) - \frac{\sum_{j=1}^{N+1} f_k(t, X_j)}{N+1}\right)^2 \le \varepsilon$$

where ε is a tolerance (largest error accepted).

The objective function is minimized in the sense of least squares as a measure of model fitting quality for the experimental data.

Fig. 6 presents a least-squares sum surface for different values of the adjusting parameters K_i and $(t_R)_i$.

It is seen that in the middle part of the space the surface of the least-squares sum shows a widening minimum, which extends further to increasing the values of K_i and $(t_R)_i$. Finding a global minimum on such a flat surface is a difficult task. The polytope algorithm found a better minimum than the Levenberg–Marquardt method. The polytope minimization method converged to a solution with the residual function value about 10% lower than the one yielded by the Levenberg–Marquardt method.

The solid lines in Fig. 7 show the decreases of moisture mass in the samples according to formula (15) for the five narrow ranges of the air relative humidity changes. The dots represent the moisture decreases determined experimentally. The bars placed on the experimental data indicate the possible error of the measurements or the area of confidence interval estimated for a 95% confidence level.

Accuracy of the correlation depends on the choice of the parameters K_i and $(t_R)_i$, on which the coefficient of diffusion $(D_{\text{eff}})_i$ and the coefficient of the convective gas-side transfer k_i depends. Different values of the mean diffusion coefficients are obtained for the different narrow ranges of the air humidity change, and, indirectly, on the moisture concentration C, as estimated on the basis of the desorption isotherm (Fig. 4).

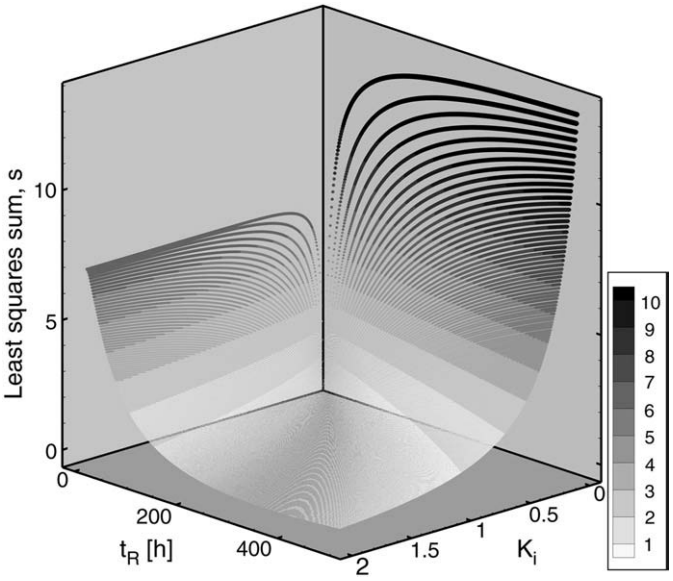

Fig. 6. Least-squares sum as a function of parameters K_i and $(t_R)_i$.

Adsorption/desorption or humidification processes involve the diffusion of one gas component (vapor) through another non-diffusing (stagnant) gas component (air). The steady state diffusion of one gas through a second stagnant gas can be replaced by convective mass transfer when using the "film concept" or "film theory". The film concept has proved that the convective mass transfer coefficient is related to the mass diffusivity, but is not directly proportional. It is rather raised to an exponent varying from 0.5 to 1.0, [45].

In our case, the stagnant gas (air) concerns not only the external film, but is extended into the capillary cell. Having in mind the condition of mass continuity at the body surface (i.e. at the end of the capillary cell), we can state that the coefficients of diffusion inside and outside the capillary cell ought to be related to each other. Thus, the coefficient of the convective gas-side transfer k_i can be related to the diffusion coefficient $(D_{\text{eff}})_i$ inside the capillary cell. In other words, both coefficients can be dependent on moisture content C. Only in the case of a fully-saturated porous material, when the surface of the body is wet, the rate of evaporation is independent from the internal moisture transport, and is solely dependent on external conditions: vapor partial pressure, temperature, and geometry of the system. In the theory of drying (see Ref. [40]), this period is called *the constant drying rate period*. In the second drying period, called *the falling drying rate period*, when the evaporation takes place inside the capillary-pores, the rate of moisture removal depends on the internal mass transport conditions: the coefficients influencing the rate of diffusion are dependent on the moisture content C.

As seen in Fig. 7, the correlation of the desorption curves obtained from the linear model with the experimental ones for the five narrow ranges of the air humidity change is partly satisfactory. Four of the five experiments are not described accurately by the linear diffusion equation. The disagreement concerns mainly the final stage of the diffusion process. The experimental plots show that on this stage the true diffusion process proceeds more slowly than the theoretical ones. Therefore, the experimental curves were next correlated with the non-linear diffusion model provided by Eq. (9).

Numerical results of the non-linear initial-boundary value problem, applied to the five cycles of the narrow air humidity changes, are presented graphically in Fig. 8.

It can be seen that moisture-dependent diffusion coefficients assure a better consistence between of the model desorption curves and the experimental data. The coefficient for the broad range of the relative air humidity change was constructed in a similar way as those for five narrow ranges of the air relative humidity change.

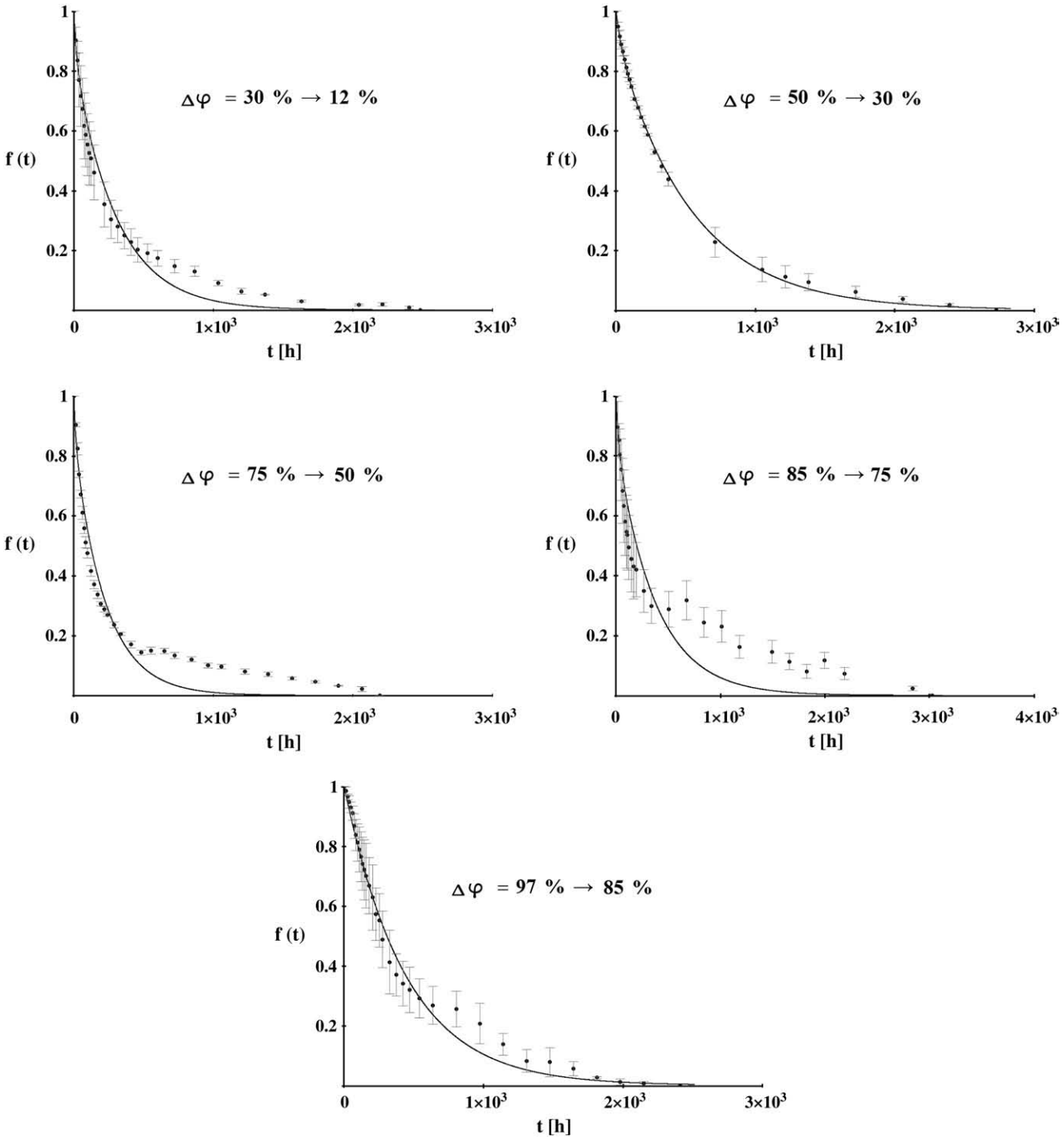

Fig. 7. Visualization of adjusting the theoretical curves with the experimental data, according to formula (15) for the five narrow ranges of the air relative humidity changes.

Fig. 9 illustrates the space evolution of moisture desorption in time for the process $\Delta\varphi$: 97% → 0%, calculated on the basis of the non-linear model.

It is seen that the distribution of moisture content in the sample becomes more and more uniform in the course of the desorption process.

Fig. 10 presents a graphical illustration of the diffusion coefficients as a function of the moisture content C for both narrow and broad ranges of the air relative humidity change.

From Fig. 10 we see that the diffusion coefficients differ from each other in several intervals of the air humidity change. Fig. 11 illustrates average values of the diffusion coefficient in several intervals.

It is seen that the average values of the diffusion coefficient are different in several intervals of the air relative humidity changes. The average diffusion coefficient, taken from the five narrow intervals, differs insignificantly from the average of that one for the broad interval $\Delta\varphi$: 97% → 0%. It means that the desorption process rate depends not only on the moisture content but on the magnitude of the interval $\Delta\varphi$ as well.

Fig. 12 presents the decrease of moisture concentration in the mortar sample for the broad range of the air relative humidity change. The theoretical curves obtained from the solution of the non-linear diffusion equation (solid line) and the linear diffusion equation (dotted line) are compared with the experimental data for $\Delta\varphi$: 97% → 0%.

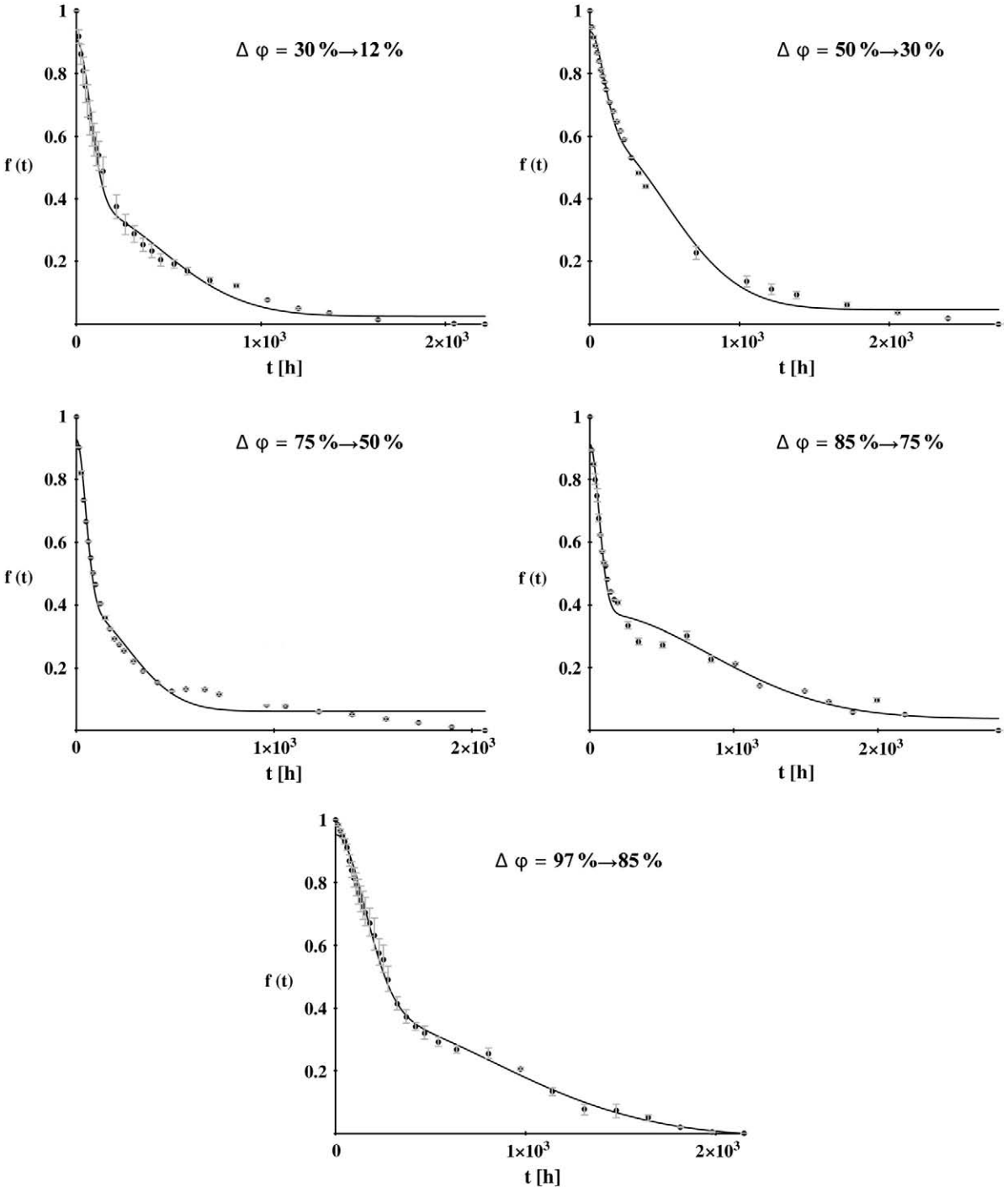

Fig. 8. Visualization of adjusting the theoretical curves with the experimental data for the five narrow ranges of the air relative humidity changes by applying the non-linear model of diffusion.

The results presented in Fig. 12 show clearly that the non-linear theory of diffusion reflects the experimentally realized desorption processes better than the linear one. The non-linear model fits the experimental data with excellent accuracy, while the linear one is even out of the confidence interval shown by the vertical bars for the data measured experimentally on the final stage of the desorption process.

7. Conclusions

The problem of satisfactory modeling of desorption processes in hygroscopic porous materials like the cement mortar on the basis of diffusion theory has been discussed. One of the main problems discussed in this paper concerns applicability of both linear and non-linear diffusion models for description of these processes. It was stated that the linear model could be tolerated but rather for narrow and not for broad ranges of the air relative humidity changes. The experimental material on adsorption–desorption processes in cement mortar, gathered from very long time measurements in desiccators, provided a basis for examination of this problem as well as for adequate estimation of an effective diffusion coefficient. The approximation procedure, based on the stochastic polytope algorithm, was used to correlate theoretical curves to the experimental data. The final conclusion is that the desorption processes from porous hygroscopic

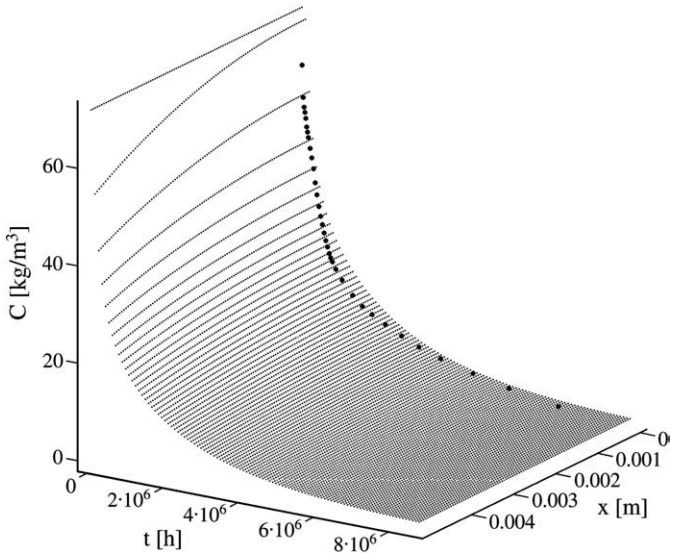

Fig. 9. Computer simulated distribution of moisture content in a sample during desorption at Δφ: 97%→0% (black points denote experimental data).

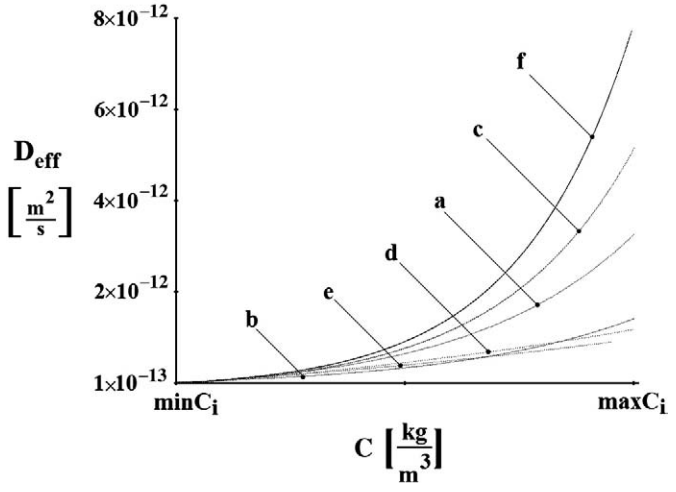

Fig. 10. Diffusion coefficient as a function of moisture content *C* for several intervals of the air humidity change: a) 30%→12%, b) 50%→30%, c) 75%→50%, d) 85%→75%, e) 97%→85%, f) 97%→0%.

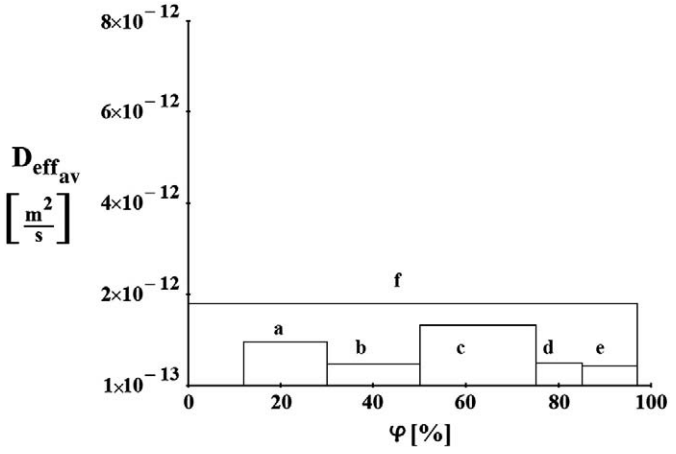

Fig. 11. Average values of the diffusion coefficient for several intervals of the air relative humidity change: a) 30%→12%, b) 50%→30%, c) 75%→50%, d) 85%→75%, e) 97%→85%, f) 97%→0%.

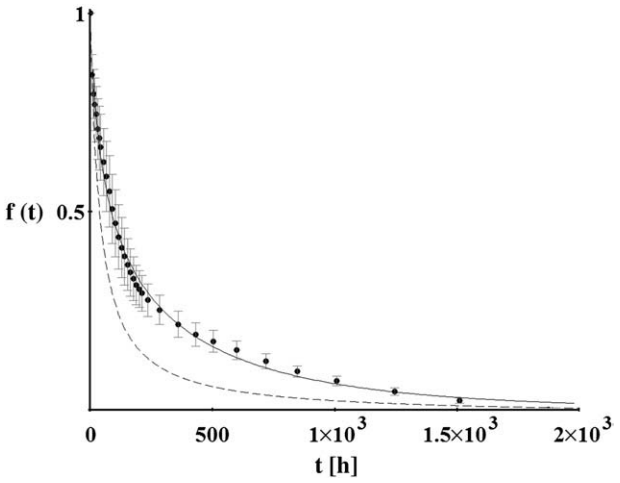

Fig. 12. Comparison of the non-linear (solid line) and the linear (dotted line) theories, correlated with experimental data (black points) for desorption at Δφ: 97%→0%.

materials like cement mortar are significantly non-linear. They can be modeled on the basis of the non-linear diffusion theory with the diffusion coefficient being a function of the moisture content. The effective diffusion coefficient, which combines diffusive transport of moisture in the adsorbed or in the gaseous phase, was constructed as a function of moisture content. It was stated that such a coefficient depends on both the moisture content and the length and location of the air relative humidity interval, which the coefficient refers to. Such dependence can be explained just by the fact that this coefficient combines transport in both the adsorbed and the gaseous phases, and the domination of a given phase is different for individual ranges of the air relative humidity. A different moisture transport proceeds in the adsorbed and in the liquid phases, as it was concluded by Andersson [46], who analyzed the moisture transport in building materials attributing coefficient D_L to liquid phase and D_V to gas phase (Fig. 13).

According to the Andersson's analysis, transport in adsorbed and gas phase differs in the course of desorption process, depending on the moisture content and thus also on the range of the air relative humidity.

Finally, we conclude that the analytical solution of the linear diffusion model can be acceptable for description of desorption processes by narrow ranges of the air relative humidity changes, however, it is unacceptable for broad ranges of the air relative humidity changes. The non-linear model with a variable diffusive coefficient $D_{eff}(C)$ provided a much more accurate correlation in all cases.

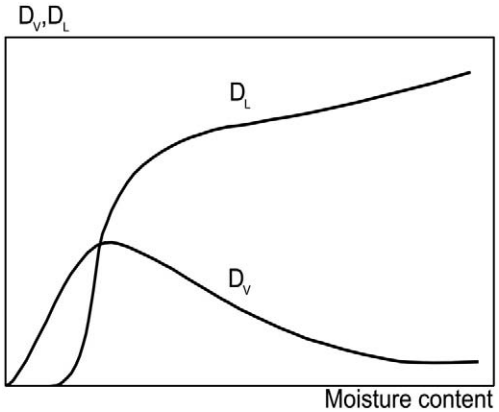

Fig. 13. Variation of moisture transfer coefficient with moisture content (Andersson, 1985).

Nomenclature

A	area of disc face, m^2
C	moisture concentration in gas phase, kg/m^3
C_s	adsorbed moisture concentration, kg/m^3
C_s^*	excess of adsorbed moisture content, kg/m^3
D	coefficient of diffusion in gas phase, m^2/s
D_s	coefficient of diffusion in adsorbed phase, m^2/s
D_{eff}	effective coefficient of diffusion, m^2/s
d	diameter of the sample, m
H	Henry's constant, –
K	parameter of correlation, –
k	coefficient of convective vapor exchange, m/s
l	half height of the sample, m
m	mass, kg
m_m	mass of moisture, kg
$m_{m\infty}$	mass of moisture at the end of desorption, kg
R	capillary radius, m
t	time, s
t_R	retardation time, s
x	spatial coordinate, m
X	two-dimensional vector, –

Greek symbols

α	reflection coefficient, –
β	expansion coefficient, –
ω_n	eigenvalues, –
δ	thickness of absorption layer, m
φ	air relative humidity, %

Indices

a	denotes air
eff	denotes effective
i	denotes number of *i*-th cycle or *i*-th iteration
m	denotes moisture
s	denotes sorption

Acknowledgements

This work was carried out as a part of the research projects no. DS 32-266/10 and DS 32-267/10 sponsored by the Poznań University of Technology and the research project no. BW-17-0302/17-01 sponsored by the West Pomeranian University of Technology.

References

[1] E. Stora, B. Bary, Qi-Chang He, On estimating the effective diffusivity properties of hardened cement pastes, Transport in Porous Media 73 (2008) 279–295.
[2] R.W. Carlson, Drying shrinkage of large concrete members, American Concrete Institute. Proceedings 33 (1937) 327–336.
[3] F.S. Rostasy, Zur Theorie der Austrocknung und des Schwindens Zementgebundener Massen, Zement – Kalk – Gips 13 (3) (1960) 93–103.
[4] N.L. Hancox, A note on the form of the rate of drying curve for cement paste and its use in analysing the drying behaviour of this material, RILEM Bulletin 36 (9) (1967) 197–201.
[5] J.A. Hanson, Effects of curing and drying environments on the splitting and tensile strength of concrete, American Concrete Institute Journal 65 (1968) 535–543.
[6] J. Kasperkiewicz, Dyfuzja wilgoci i deformacje skurczowe w betonie, PWN, Warszawa, 1972.
[7] S.E. Pihlajavaara, Notes on the drying of concrete. Helsinki (The State Institute for Technical Research, Tiedotus, Sarja III – Rakennus 74) (1963).
[8] S.E. Pihlajavaara, On the main features and methods of investigation of drying and related phenomena in concrete, Dissertation, University Helsinki (1965).
[9] Z.P. Bažant, L.J. Najjar, Drying of concrete as a nonlinear diffusion problem, Cement and Concrete Research 1 (1971) 461–473.
[10] Z.P. Bažant, L.J. Najjar, Nonlinear water diffusion in nonsaturated concrete, Materiaux et Constructions 5 (25) (1972) 3–20.
[11] B.H. Vos, Internal condensation in structures, Building Science 3 (1969) 191–206.
[12] J. Van der Kooi, Moisture transport in cellular concrete roofs, Disseration, Technische Hochschule Eindhoven (1971).
[13] K. Kiessl, K. Gertis, Isothermer Feuchtetransport in porösen Baustoffen — eine makroskopische Betrachtung der instationären Transportvorgänge, Deutscher Ausschuss für Stahlbeton H. 258 (1976) 85–110.
[14] O. Adan, H. Brocken, J. Carmeliet, H. Hens, S. Roels, C.E. Hagentoft, Determination of liquid water transfer properties of porous building materials and development of numerical assessment methods: introduction to the EC HAMSTAD project", Journal of Thermal Envelope and Building Science 27 (4) (2004) 253–260.
[15] J. Carmeliet, O. Adan, H. Brocken, R. Cerny, Ch. Hall, H. Hens, K. Kumaran, Z. Pavlik, L. Pel, S. Roels, Determination of the liquid water diffusivity from transient moisture transfer experiments, Journal of Thermal Envelope and Building Science 27 (4) (2004) 277–305.
[16] C.E. Hagentoft, O. Adan, B. Adl-Zarrabi, R. Becker, H. Brocken, J. Carmeliet, R. Djebbar, M. Funk, J. Grunewald, H. Hens, K. Kumaran, S. Roels, A. Sasic Kalagasidis, D. Shamir, Assessment method of numerical prediction models for combined heat, air and moisture transfer in building components. Benchmarks for one-dimensional cases, Journal of Thermal Envelope and Building Science 27 (4) (2004) 327–352.
[17] S. Roels, O. Adan, H. Brocken, J. Carmeliet, R. Cerny, Ch. Hall, H. Hens, K. Kumaran, Z. Pavlik, L. Pel, R. Plagge, A comparison of different techniques to quantify moisture content profiles in porous building material, Journal of Thermal Envelope and Building Science 27 (4) (2004) 261–276.
[18] S. Roels, O. Adan, H. Brocken, J. Carmeliet, R. Cerny, Ch. Hall, H. Hens, K. Kumaran, Z. Pavlik, L. Pel, R. Plagge, Interlaboratory comparison of hygric properties of porous building materials, Journal of Thermal Envelope and Building Science 27 (4) (2004) 307–325.
[19] H. Garbalińska, Measurement of the mass diffusivity in cement mortar: use of initial rates of water absorption, International Journal of Heat and Mass Transfer 45 (6) (2002) 1353–1357.
[20] H. Garbalińska, Isothermal coefficients of moisture transport for porous building material, Scientific Works of Szczecin University of Technology Bulletin No. 571, (2002) Szczecin (in Polish).
[21] H. Garbalińska, Application of √t-type, logarithmic and half-time methods in desorptive measurements of diffusivity in narrow humidity ranges, Cement and Concrete Research 36 (2006) 1294–1303.
[22] S. Basau, U.S. Shivhare, A.S. Mujumdar, Models for sorption isotherms for foods: a review, Drying Technology 24 (8) (2006) 917–930.
[23] X.D. Chen, Moisture diffusivity in food and biological materials, Drying Technology 25 (7–8) (2007) 1203–1213.
[24] G. Dali, D.K. Apar, B. Özbek, Estimation of moisture diffusivity of okra in microwave drying, Drying Technology 25 (9) (2007) 1445–1450.
[25] Y.I. Babenko, E.V. Ivanov, Extraction from a capillary with a variable diffusion coefficient, Theoretical Foundations of Chemical Engineering 42 (4) (2008) 341–346.
[26] D. Marquardt, An algorithm for least-squares estimation of nonlinear parameters, SIAM Journal of Applied Mathematics 11 (1963) 431–441.
[27] H. Garbalińska, Assessment of nonlinearity of moisture diffusion in cement mortar, Archives of Civil Engineering vol. 42 (1) (1996) 19–28.
[28] H. Garbalińska, Feuchtediffusionskoeffizienten von Zementmörteln mit verschiedenen Wasserzementwerten. Bauphysik (1998) Jg. 20 H. 2, 56–65.
[29] H. Garbalińska, Application of the logarithmic procedure to absorption measurements of mass diffusivity for cement mortars, Research Journal Heat and Mass Transfer 40 (2004) 963–972.
[30] H. Garbalińska, Comparative analysis of desorptive methods used for mass diffusivity estimation, Acta Scientiarum Polonorum-Architectura 5 (2) (2006) 3–15.
[31] H. Garbalińska, Study on coefficients of capillary flow by means of Wet-Cup Method and Inverse-Wet-Cup Method, Archives of Civil Engineering vol. 47 (4) (2001) 539–558.
[32] H. Garbalińska, Kapillarer Wassertransport in Zementmörtel. Experimentelle Bestimmung der Koeffizienten des kapillaren Saugens, Bauphysik (2002) Jg. 24 H. 2, 87–92.
[33] H. Garbalińska, A. Wygocka, Prüfkörperabdichtung und der Wasserabsorptionskoeffizient von mit Polypropylenfasern modifizierten Zementmörteln, Bauphysik (2007) Jg. 29 H. 6, 436–441.
[34] A.M. Neville, Concrete Properties (in Polish), Polski Cement, Kraków, 2000.
[35] PN-EN 196-1:2006 Methods of testing cement. Determination of strength (in Polish).
[36] J. Kropp, Karbonatisierung und Transportvorgänge in Zementstein, Dissertation, Universität Karlsruhe 1983.
[37] G.A. Aksielrud, M.A. Altshuler, Transport of mass in porous media, PWN, Warszawa, 1987 (in Polish).
[38] P.G. Shewmon, Diffusion in solids, McGraw-Hill, New York, 1963.
[39] W. Dudziak, S.J. Kowalski, Theory of diffusion for solids, International Journal of Heat and Mass Transfer 32 (11) (1989) 2005–2013.
[40] S.J. Kowalski, Thermomechanics of drying processes, Springer Velag, Heidelberg, Berlin, 2003.
[41] C.W. Gear, Numerical initial value problems in ordinary differential equations, Prentice-Hall, Englewood Cliffs, NJ, 1971.
[42] J.J. More, B.S. Garbow, K.E. Hillstrom, User guide for MINPACK-I, Argonne National Laboratory Report ANL-80-74, Argone, III, (1980).
[43] J.A. Nelder, R. Mead, A simplex method for function minimization, Computer Journal 7 (1965) 308–313.
[44] P.E. Gill, W. Murray, M. Wright, Practical Optimization, Academic Press, New York, 1981.
[45] J.R. Welty, C.E. Wicks, R.E. Wilson, Fundamentals of momentum, heat, and mass transfer, second ed.John Wiley & Sons, New York, 1976.
[46] A.Ch. Andersson, Verification of calculation methods for moisture transport in porous building materials, SCBR (Document Swedish Council for Building Research D6, Stockholm, 1985.